INTERNATIONAL ATOMIC ENERGY AGENCY
UNITED NATIONS EDUCATIONAL, SCIENTIFIC AND CULTURAL ORGANIZATION
INTERNATIONAL CENTRE FOR THEORETICAL PHYSICS
I.C.T.P., P.O. BOX 586, 34100 TRIESTE, ITALY, CABLE: CENTRATOM TRIESTE

SMR/697
9-Mag.Mult.

RESEARCH WORKSHOP ON CONDENSED MATTER PHYSICS
(21 June - 3 September 1993)

WORKING GROUP ON MAGNETIC MULTILAYERS
(9 - 13 August 1993)

SEGREGATION EFFECTS ON THE MAGNETIC PROPERTIES OF BIMETALLIC MULTILAYERS

J.L. MORAN LOPEZ
Universidad Autonoma de San Luis Potosi
Instituto de Fisica
Alvaro Obregon 64
78000 San Luis Potosi
MEXICO

These are preliminary lecture notes, intended only for distribution to participants

MAIN BUILDING STRADA COSTIERA, 11 TEL 22401 TELEFAX 224163 TELEX 460392 ADRIATICO GUEST HOUSE VIA GRIGNANO, 9 TEL. 224241 TELEFAX 224531 TELEX 460449
MICROPROCESSOR LAB. VIA BEIRUT, 31 TEL. 224471 TELEFAX 224163 TELEX 460392 GALILEO GUEST HOUSE VIA BEIRUT, 7 TEL. 22401 TELEFAX 224559 TELEX 460392

SEGREGATION EFFECTS ON THE MAGNETIC PROPERTIES OF BIMETALLIC MULTILAYERS

J.L. Morán-López, A. Díaz-Ortíz, and F. Aguilera-Granja

Instituto de Física

Universidad Autónoma de San Luis Potosí

San Luis Potosí, S.L.P., México

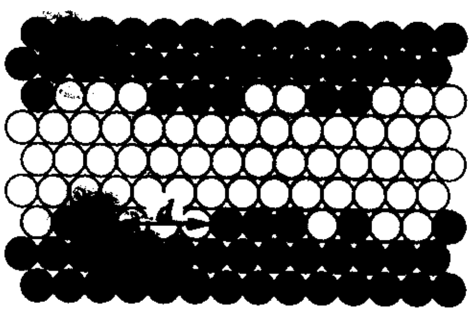

PHYSICAL REVIEW B VOLUME 45, NUMBER 21 1 JUNE 1992-I

Structural study of cobalt-copper multilayers by NMR

C. Mény and P. Panissod
Institut de Physique et Chimie des Matériaux (GEMME), Université Louis Pasteur, 4 rue Blaise Pascal, 67070 Strasbourg, France

R. Loloee
Department of Physics and Astronomy, Center for Fundamental Materials Research, Michigan State University, East Lansing, Michigan 48874

(Received 9 December 1991)

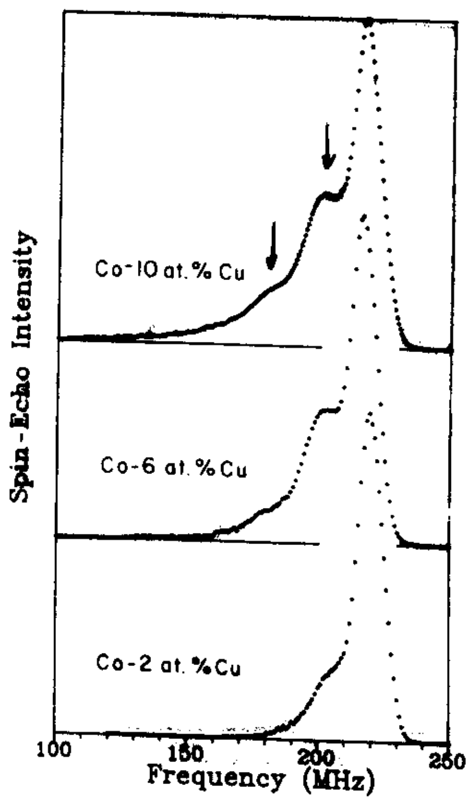

FIG. 1. ^{59}Co NMR spectra of cobalt-copper alloys with 2, 6, and 10 at. % of copper. The main line is attributed to Co with 12 Co nearest neighbors and each successive satellite to the successive substitution of Cu for Co in the vicinity of Co.

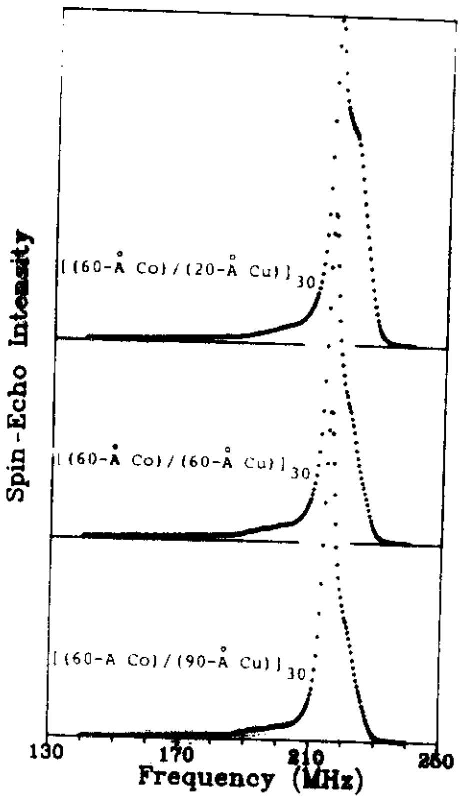

FIG. 2. NMR spectra of the multilayers with 60 Å of cobalt. The main line is attributed to fcc Co, the two upper lines to hcp Co, and the satellites at low frequencies to Co at the interfaces

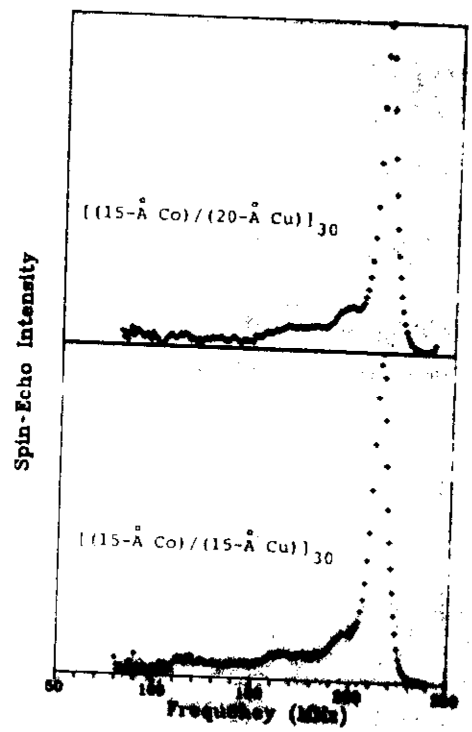

FIG. 3. NMR spectra of the multilayers with 15-Å cobalt thickness. The main line is attributed to fcc Co and the satellites to Co at the interfaces of the multilayers.

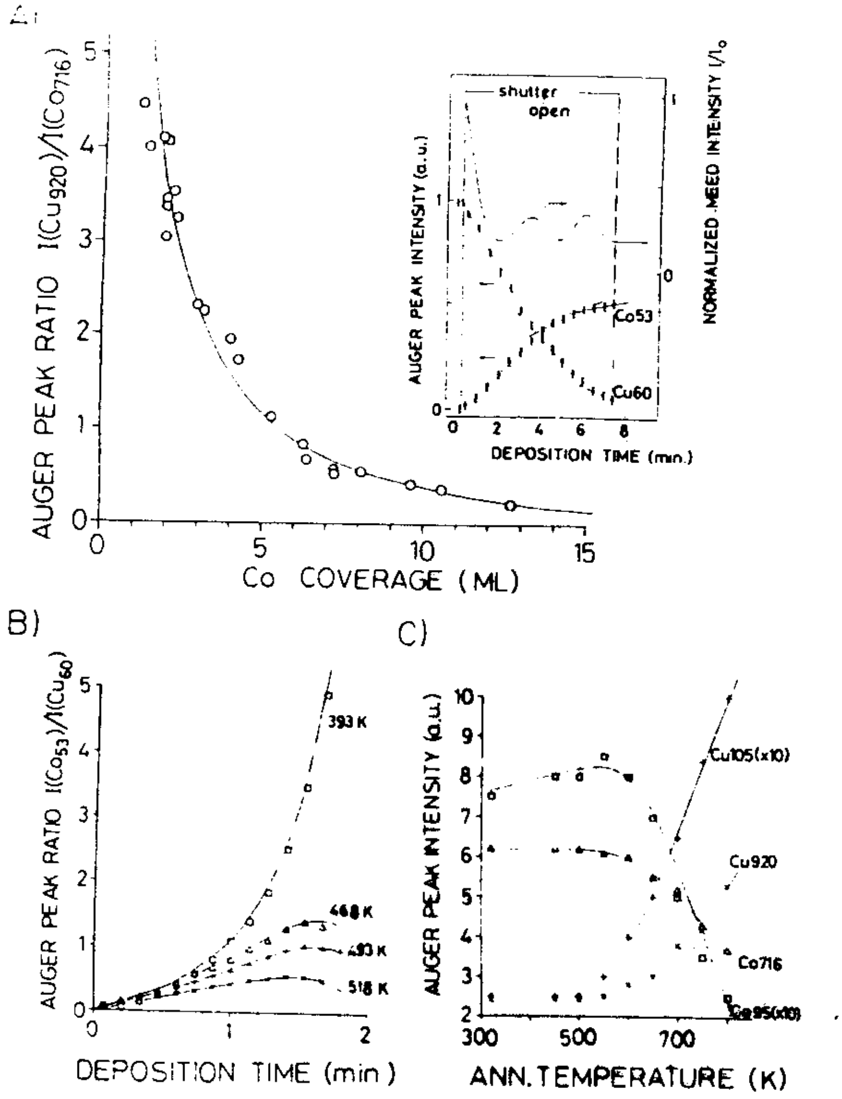

Fig. 2. (a) Ratio of the peak-to-peak intensities of the Auger peaks of Cu at 920 eV and Co at 716 eV as a function of the number of Co layers deposited at 420 K on a Cu(100) substrate. The inset shows the evolution of the low energy Auger peaks of Co and Cu displaying the characteristic breaks at completion of the first few layers; (b) ratio of the low energy Auger peaks of Co and Cu during deposition at different substrate temperatures; (c) evolution of the Auger peaks during annealing of 2.7 ML of Co 1 min at various temperatures.

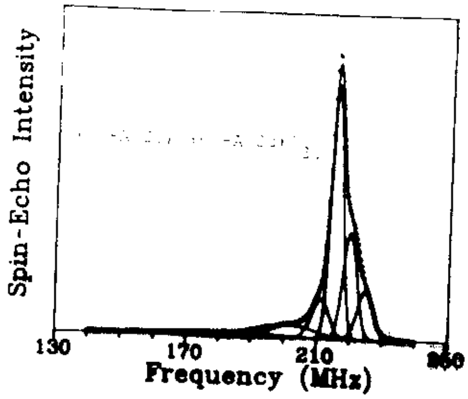

FIG. 5. Example of coarse Gaussian decomposition of a multilayer NMR spectrum.

TABLE III. Number of cobalt atoms in the interfaces of the multilayers in units of full Co monolayers per interface (FML).

Sample	Co in the interface (FML)
(15-Å Co)/(15-Å Cu)	1.7
(15-Å Co)/(20-Å Cu)	1.7
(60-Å Co)/(20-Å Cu)	3.0
(60-Å Co)/(60-Å Cu)	3.8
(60-Å Co)/(90-Å Cu)	3.5

Multilayer cross section

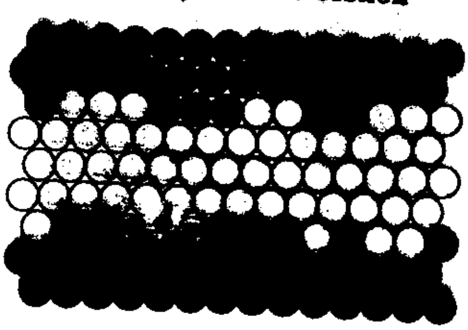

Invited paper

Influence of the growth conditions on the magnetic properties of fcc cobalt films: from monolayers to superlattices

J.J. de Miguel, A. Cebollada, J.M. Gallego, R. Miranda

Departamento de Física de la Materia Condensada, Universidad Autónoma de Madrid, Cantoblanco, 28049 Madrid, Spain

C.M. Schneider, P. Schuster and J. Kirschner

Institut für Experimentalphysik, Freie Universität Berlin, Arnimallee 14, W-1000 Berlin 33, Germany

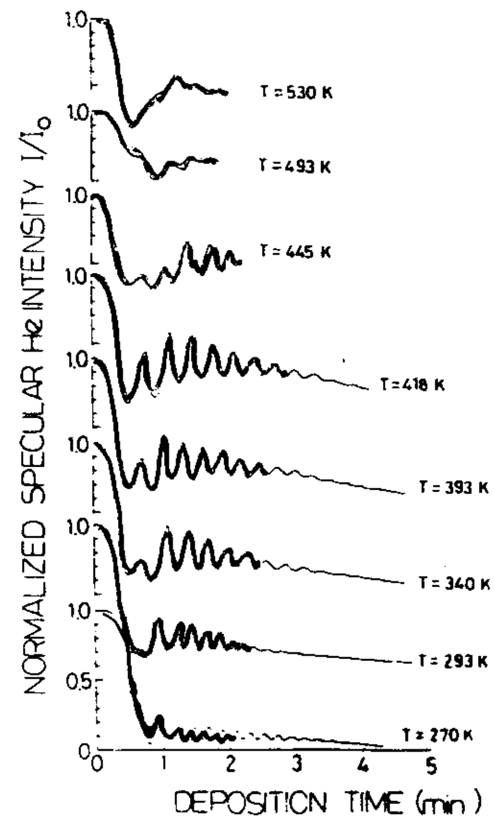

Fig. 1. Temperature dependence of the TEAS oscillations observed during deposition of Co on Cu(100) under destructive interference conditions.

TEAS

Thermal Energy Atom Scattering.

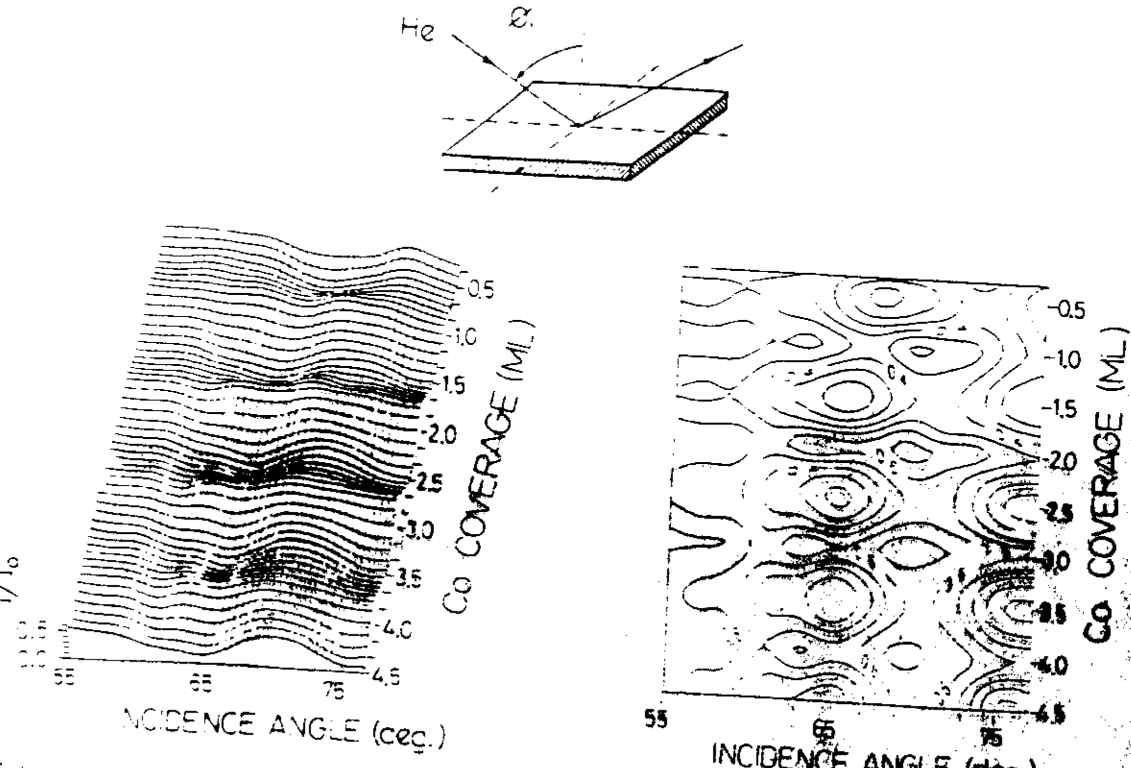

Fig. 3 (a) Specular intensity of TEAS as a function of the azimuthal angle of incidence and the deposited coverage for Co/Cu(...) ... plot of the data in (a). For constant angle of incidence, maxima in the reflected intensity appear at completion of every ... layer. For any given coverage, there is a rocking curve reflecting the interference conditions (e.g. vertical distances, density of atomic terraces. The evaporation was carried out at 420 K.

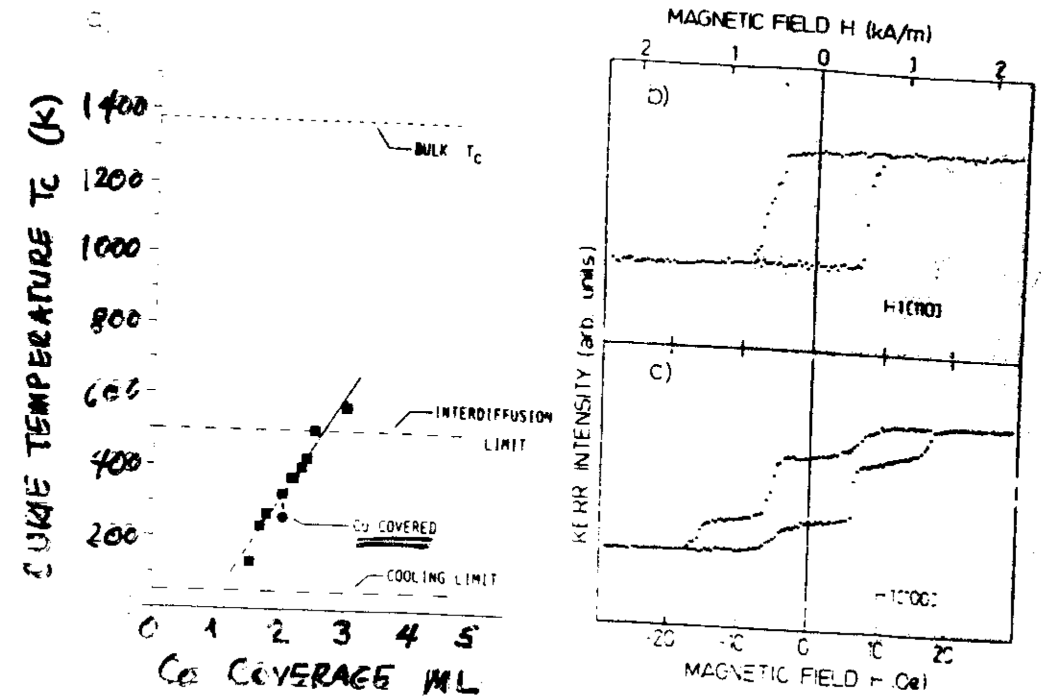

Fig. 4 (a) Coverage dependence of the Curie temperature for ultrathin films of Co/Cu(100). T_c was determined from SMOKE hysteresis curves recorded as a function of the sample temperature with the magnetizing field in-plane and normal to the surface plane. There was no component of the magnetization perpendicular to the plane. The filled circle is a data point taken after covering 2 ML of Co with a Cu overlayer; (b) hysteresis loops for 4 ML of Co/Cu(100) recorded at 300 K with the external magnetic field applied in two high-symmetry directions of the film plane.

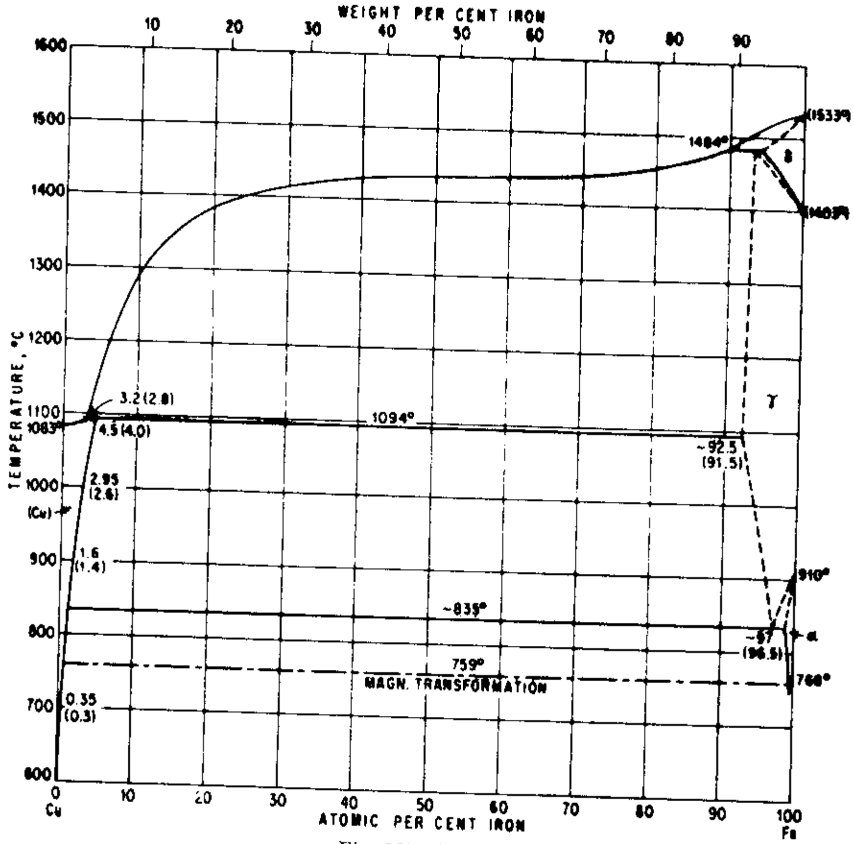
WEIGHT PER CENT IRON
ATOMIC PER CENT IRON
TEMPERATURE, °C
1484°
(1533°)
(1403°)
δ
γ
3.2 (2.8)
4.5 (4.0)
1083°
1094°
~92.5
(91.5)
2.95
(2.6)
(Cu)
1.6
(1.4)
~835°
910°
~97
(96.5)
α
759°
MAGN. TRANSFORMATION
768°
0.35
(0.3)
Cu
Fe

Fig. 337. Cu-Fe

PHYSICAL REVIEW B VOLUME 17, NUMBER 2 15 JANUARY 1978

Clustering in Cu-Ni alloys: A diffuse neutron-scattering study

J. Vrijen
Netherlands Energy Research Foundation ECN, Petten, The Netherlands

S. Radelaar
Physics Laboratory, Rijksuniversiteit Utrecht, Utrecht, The Netherlands

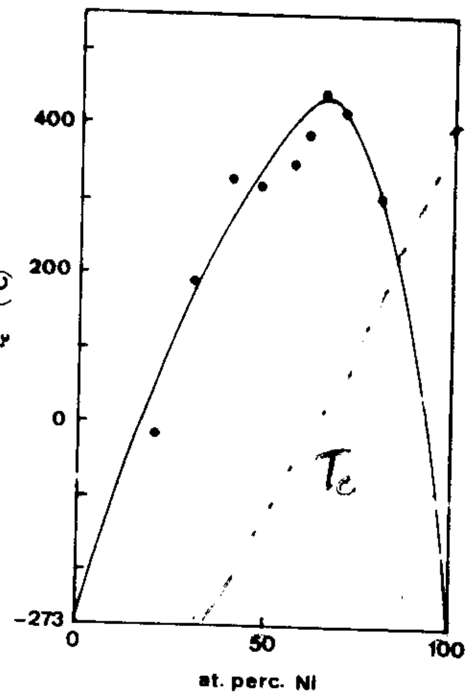

FIG. 11. Miscibility gap in Cu-Ni, calculated for the various compositions from the diffuse-neutron-scattering results with the model of Clapp and Moss. The line is drawn to guide the eye.

E

PHYSICS REPORTS (Review Section of Physics Letters) 153, No. 6 (1987) 331–399. North-Holland, Amsterdam

MAGNETISM AND SPATIAL ORDER IN TRANSITION METAL ALLOYS: EXPERIMENTAL AND THEORETICAL ASPECTS

M.C. CADEVILLE

Laboratoire de Magnetisme et de Structure Electronique des Solides (UA CNRS n° 306), Université Louis Pasteur, 4, rue Blaise Pascal, 67070 Strasbourg Cedex, France

J.L. MORÁN-LÓPEZ

Instituto de Fisica, Universidad Autonoma de San Luis Potosí, 78000 San Luis Potosí, S.L.P., México

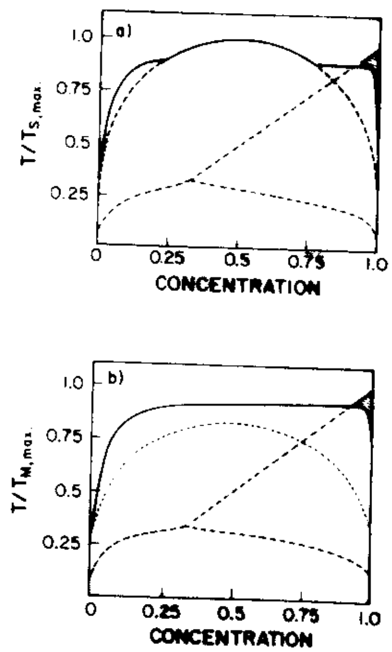

Fig. 30. Phase diagram for segregating alloys with one magnetic component as obtained in the Bragg–Williams approximation [83]. The dashed lines are the unperturbed transition temperatures.

$$kT_c = \frac{W}{2 \ln \frac{z}{z-2}}$$

Magnetic Phase Transition in Two-Dimensional Ultrathin Fe Films on Au(100)

W. Dürr,[1] M. Taborelli,[2] O. Paul,[2] R. Germar,[1] W. Gudat,[1] D. Pescia,[1] and M. Landolt[2]
[1]*Institut für Festkörperforschung der Kernforschungsanlage Jülich, 5170 Jülich, Federal Republic of Germany*
[2]*Laboratorium für Festkörperphysik der Eidgenössische Technische Hochschule Zürich, 8093 Zürich, Switzerland*
(Received 22 September 1988; revised manuscript received 22 November 1988)

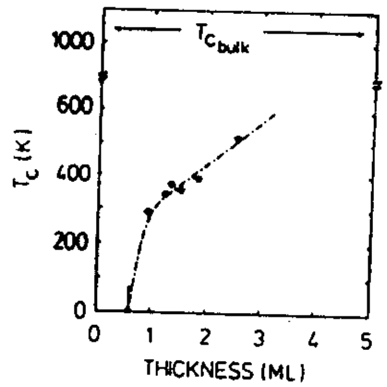

FIG. 1. Thickness dependence of the Curie temperature T_C as determined by spin-polarized secondary electron emission; the dashed curve is a guide to the eye.

- The phese transition is not sharp.
- there is a characteristic tail above T_C

The problem
- contamination
- imperfection

VOLUME 59, NUMBER 21 PHYSICAL REVIEW LETTERS 23 NOVEMBER 1987

Magnetism of Epitaxial bcc Iron on Ag(001) Observed by Spin-Polarized Photoemission

M. Stampanoni, A. Vaterlaus, M. Aeschlimann, and F. Meier
Laboratorium für Festkörperphysik, Eidgenössiche Technische Hochschule Zürich–Hönggerberg, CH-8093 Zürich, Switzerland
(Received 11 September 1987)

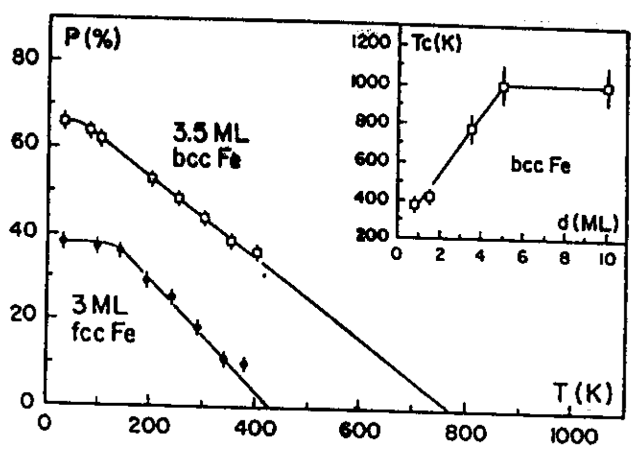

FIG. 2. Temperature dependence of the saturation polarization of a 3.5-ML-thick epitaxial bcc Fe film on Ag(001) and a 3-ML fcc Fe film on Cu(001). Inset: Thickness dependence of the Curie temperature of the bcc Fe films.

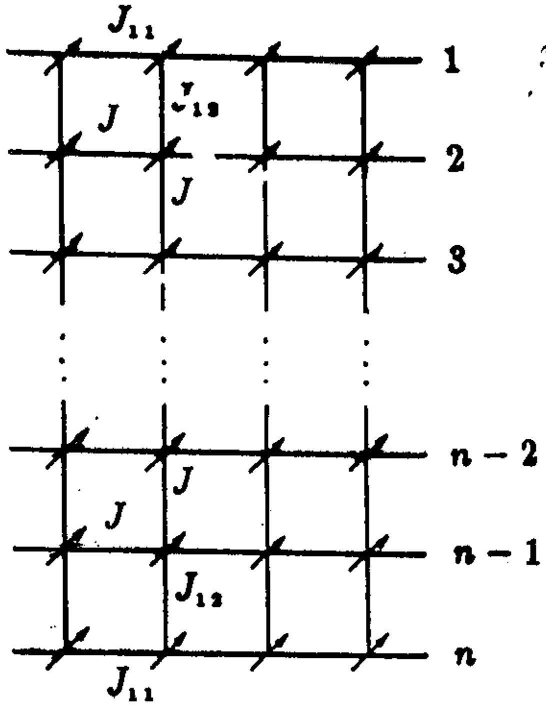
J_{11}
J_{12}
J
J
1
2
3
$n-2$
J
J
$n-1$
J_{12}
n
J_{11}

The free energy

$$F = N_{11} \left\{ \sum_{i=1} \left[-\frac{z_0}{2} J_{ii} \eta_i^2 - z_1 J_{i,i+1} \eta_i \eta_{i+1} \right] + kT \sum_{i=1} \left[\frac{1+\eta_i}{2} \ln\left(\frac{1+\eta_i}{2}\right) + \frac{1-\eta_i}{2} \ln\left(\frac{1-\eta_i}{2}\right) \right] \right\}$$

The equilibrium values of η_i are obtained by minimizing F:

$$-2\left(z_0 J_{00} \eta_0 + z_1 J_{01} \eta_1 \right) + kT \ln\left(\frac{1+\eta_0}{1-\eta_0} \right) = 0$$

$$\vdots$$

$$-2\left(z_1 J_{i-1} \eta_{i-1} + z_0 J_{ii} \eta_i + z_1 J_{i+1} \eta_{i+1} \right) + kT \ln\left(\frac{1+\eta_i}{1-\eta_i} \right) = 0$$

Close to the Curie temperature, we can linearize the η_p and the coupled set of equations can be written:

$$\hat{A}\,\hat{\eta} = 0$$

$$A_{mn} = (kT_{cs} - z_0 J_{mn})\,\delta_{mm} - z_1 J_{mn}(\delta_{m+1,n} + \delta_{n,m+1})$$

For semi-infinite systems the critical values of J_{mn} leading to the special transition $T_{cs} = T_c = zJ$ are obtained from

$$\det \hat{A} = 0$$

To calculate the determinant of the infinite matrix one first calculates the determinant of a $n \times n$ matrix and then take the limit $n \to \infty$

Semi-infinite surfaces.

Aguilera-Granja and ML.

Phys. Rev. B 31, 7146 (1985)

If $T_{cs} > T_c$ one obtains its value from

$$
\begin{vmatrix}
x-a & -c & 0 & 0 & \cdots \\
-c & x-b & -1 & 0 & \\
0 & -1 & x & -1 & \cdots \\
0 & 0 & -1 & x & -1 \\
\vdots & & & &
\end{vmatrix} = 0 \qquad (1)
$$

$$
x = \frac{kT_{cs} - z_0 J}{z_1 J}, \qquad a = \frac{z_0 (J_{11} - J)}{z_1 J}
$$

$$
b = \frac{z_0 (J_{22} - J)}{z_1 J} \qquad c = \frac{J_{12}}{J}
$$

The eq (1) can be written

$$
(x-a)\left[(x-b)\frac{\mathcal{D}_{n-2}}{\mathcal{D}_{n-3}} - 1\right] - c^2 \frac{\mathcal{D}_{n-2}}{\mathcal{D}_{n-3}} = 0
$$

$$
\mathcal{D}_m = \begin{vmatrix}
x & -1 & 0 & 0 & \cdots \\
-1 & x & -1 & 0 & \\
0 & -1 & x & -1 & \\
\vdots & & & &
\end{vmatrix}
$$

The determinant $\mathcal{D}_m$ has the property

$$\frac{\mathcal{D}_m}{\mathcal{D}_{m-1}} = x - \cfrac{1}{\cfrac{\mathcal{D}_{m-1}}{\mathcal{D}_{m-2}}}$$

for $m \to \infty$ $\quad \gamma = \frac{\mathcal{D}_m}{\mathcal{D}_{m-1}}$ and

$$\gamma^2 - x\gamma + 1 = 0$$

Thus T_{cs} is obtained from

$$b x^3 - (1 - c^2 + 2ab + b^2) x^2 + [2a(ab - c^2)(a + 2b)] x - a^2 - (ab - c)^2 = 0$$

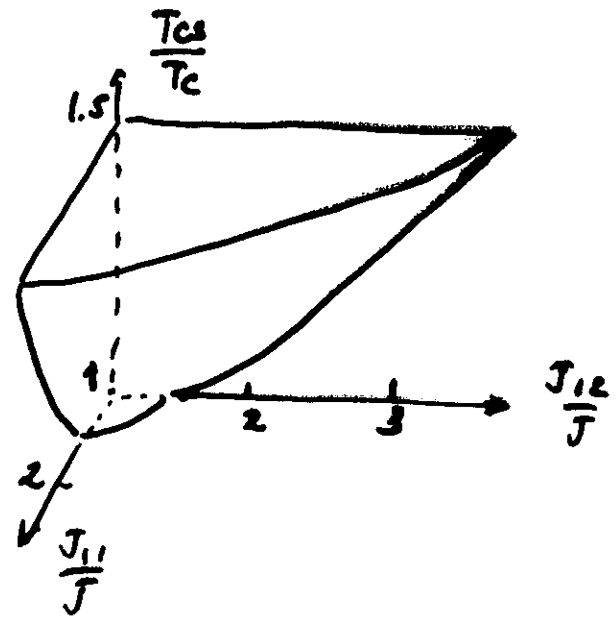

In the case $J_{mn} \neq J$ $m, n = 1, 2$

$$(z_0 J_{11,c} - zJ)\left[(z_0 J_{22,c} - zJ)(z_1 J)^{n-2} D_{n-2} - (z_1 J)^{n-1} D_{n-3}\right]$$

$$- (z_1 J_{12,c})^2 (z_1 J)^{n-2} D_{n-2} = 0$$

$$D_m = \begin{vmatrix} -2 & 1 & 0 & \cdots \\ 1 & -2 & 1 & \\ \vdots & & & \\ \cdot & & & \end{vmatrix} = (-1)^m (m+1)$$

for $n \geq 2$

$$\frac{zJ - z_0 J_{11,c}}{z_1 J}\left[\frac{zJ - z_0 J_{22,c}}{z_1 J} - \frac{n-2}{n-1}\right] = \left(\frac{J_{12,c}}{J}\right)^2$$

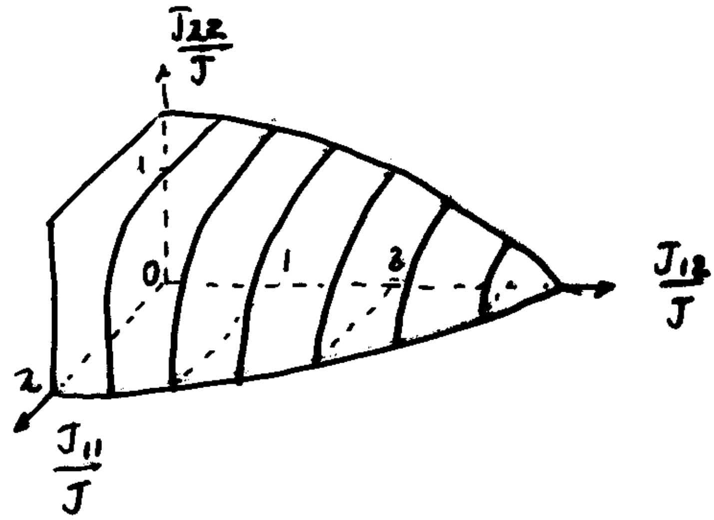

fcc (111)

$z_0 = 6$, $z_1 = 3$

Thin films.

In thin films there is only one T_c for the whole system.

$$\text{For} \quad n = \begin{cases} 1 & kT_c = z_0 J_{11} \\ 2 & kT_c = z_0 J_{11} + z_1 J_{12} \end{cases}$$

For $n=3$ $\quad x = \frac{1}{2}\left(a + \sqrt{a^2 + 8c^2}\right); \quad x = \frac{kT_c\,[illegible]}{z_1 J}$

$$a = \frac{z_0(J_{11} - J)}{z_1 J} \quad c = \frac{J_{12}}{J}$$

in general for $n \geq 4$

$$(x-a)^2 \sin n\theta - 2(x-a)c^2 \sin(n-1)\theta + c^4 \sin(n-2)\theta = 0$$

$$\tan\theta = \sqrt{4x^{-2} - 1}$$

Aguilera-Granja and ML
Solid State Commun. 74, 155 (90)

- This equation was obtained by using the cofactor expansion and the identity

$$\begin{vmatrix} 1 & -y & 0 & \cdots & 0 \\ -y & 1 & -y & \cdots & 0 \\ 0 & -y & 1 & \cdots & 0 \\ \vdots & \vdots & \vdots & \ddots & \vdots \\ 0 & 0 & 0 & \cdots & 1 \end{vmatrix}_{i \times i} = \frac{2y^{i+1}}{\sqrt{d}} \sin(i+1)\theta$$

Superlattices.

Ortiz-Saavedra, Aguilera-Granja and ML

Solid State Commun. **82**, 71 (1992)

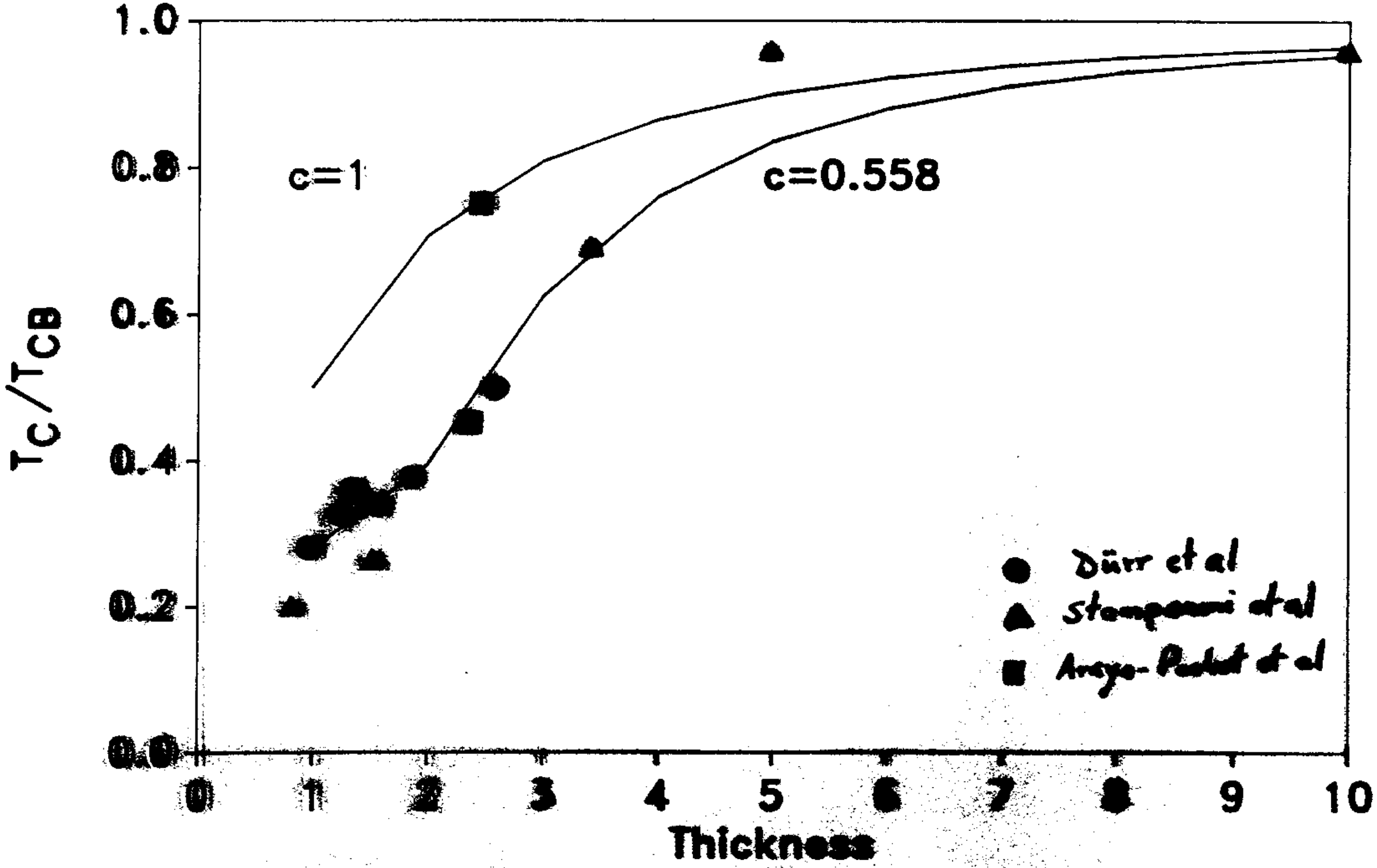

1.0
0.8
0.6
0.4
0.2
0.0
T_C/T_{CB}
0
1
2
3
4
5
6
7
8
9
10
Thickness
c=1
c=0.558
Dürr et al

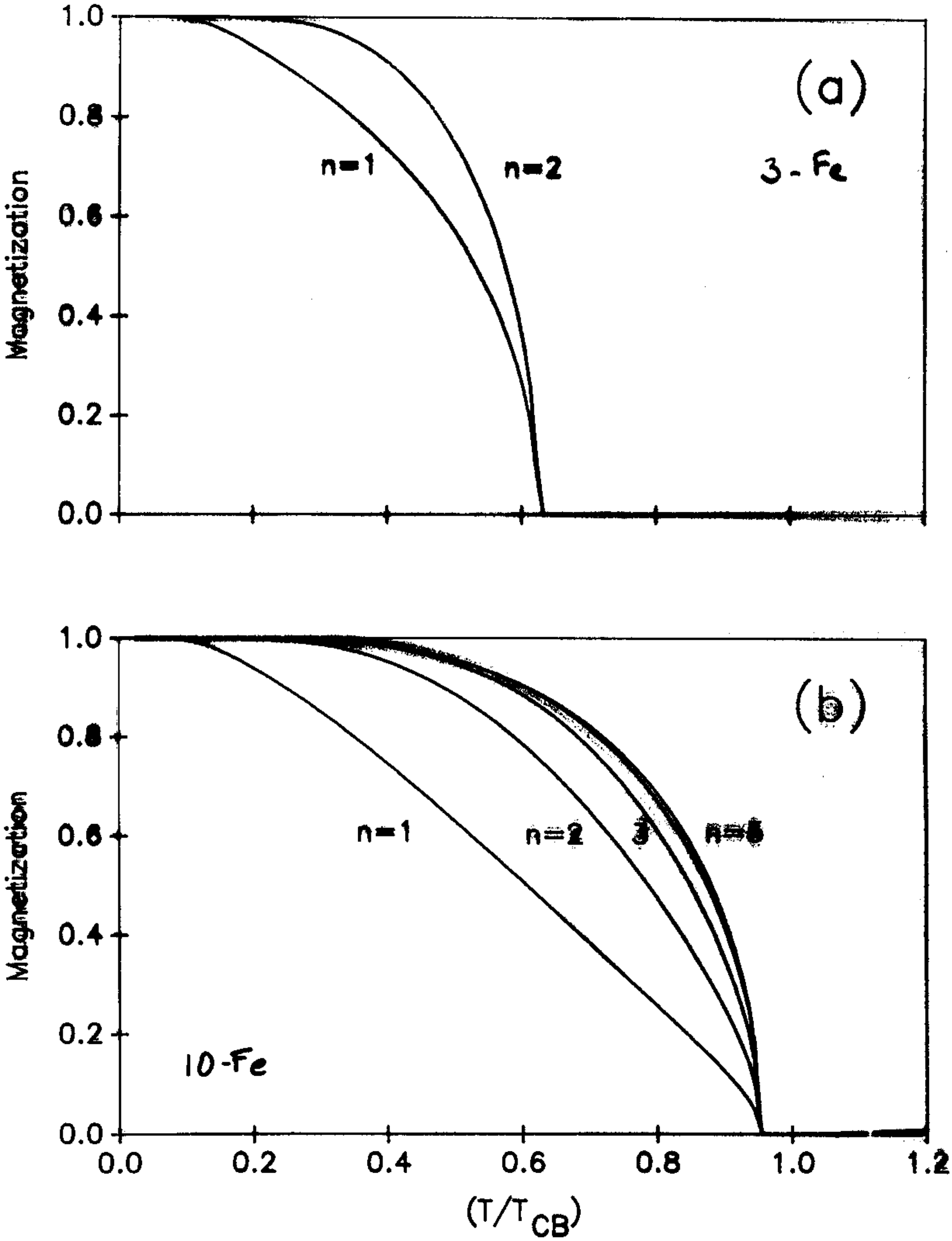

1.0
0.8
0.6
0.4
0.2
0.0
Magnetization
(a)
n=1
n=2
3 - Fe
1.0
0.8
0.6
0.4
0.2
0.0
Magnetization
(b)
n=1
n=2
3
n=5
10-Fe
0.0
0.2
0.4
0.6
0.8
1.0
1.2
(T/T_CB)

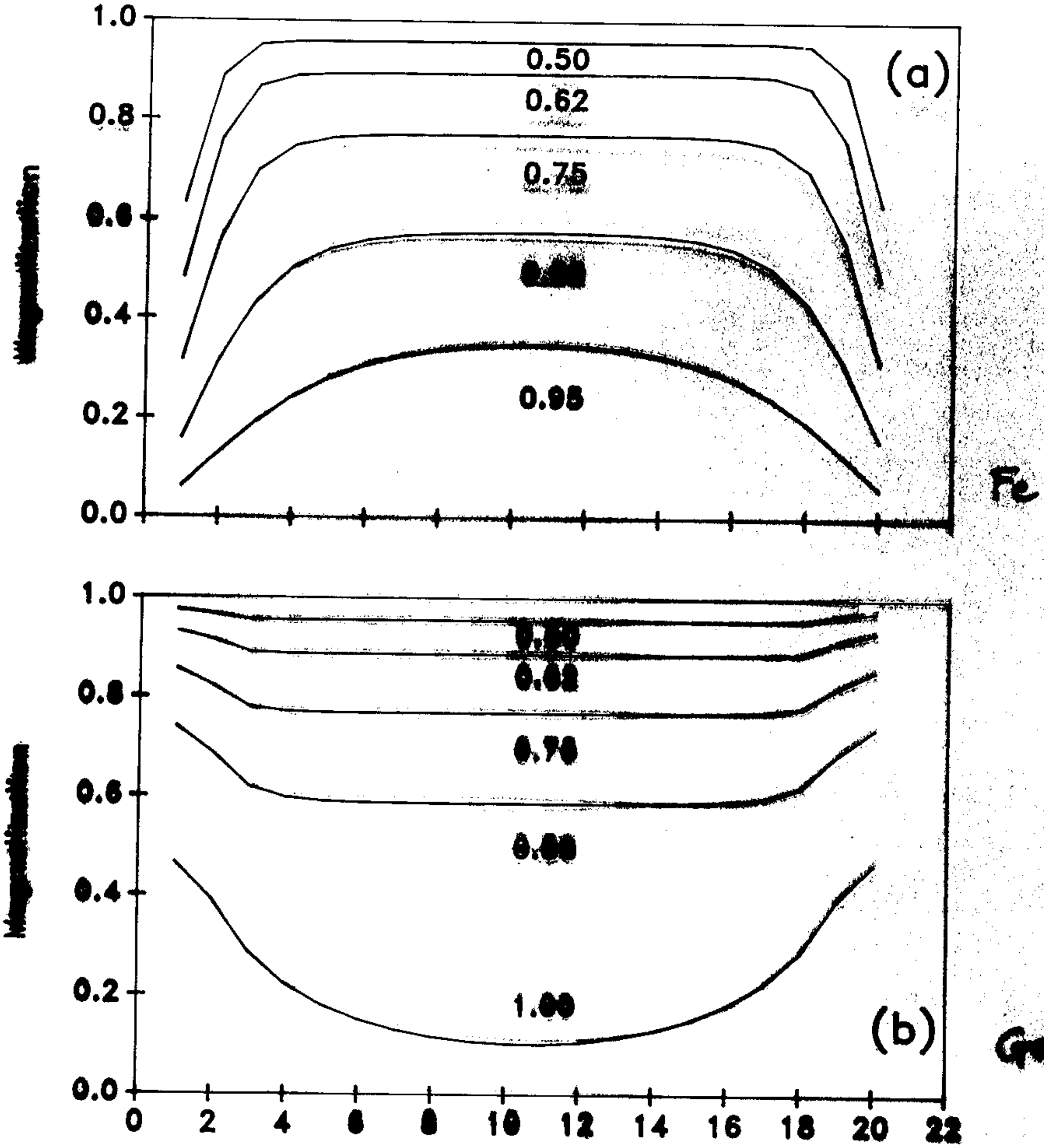

(a)
0.50
0.62
0.75
0.95
Fe
(b)
1.00
Gd.
Plane
0.0
0.2
0.4
0.6
0.8
1.0
0
2
4
10
12
14
16
18
20

NiCu <111>

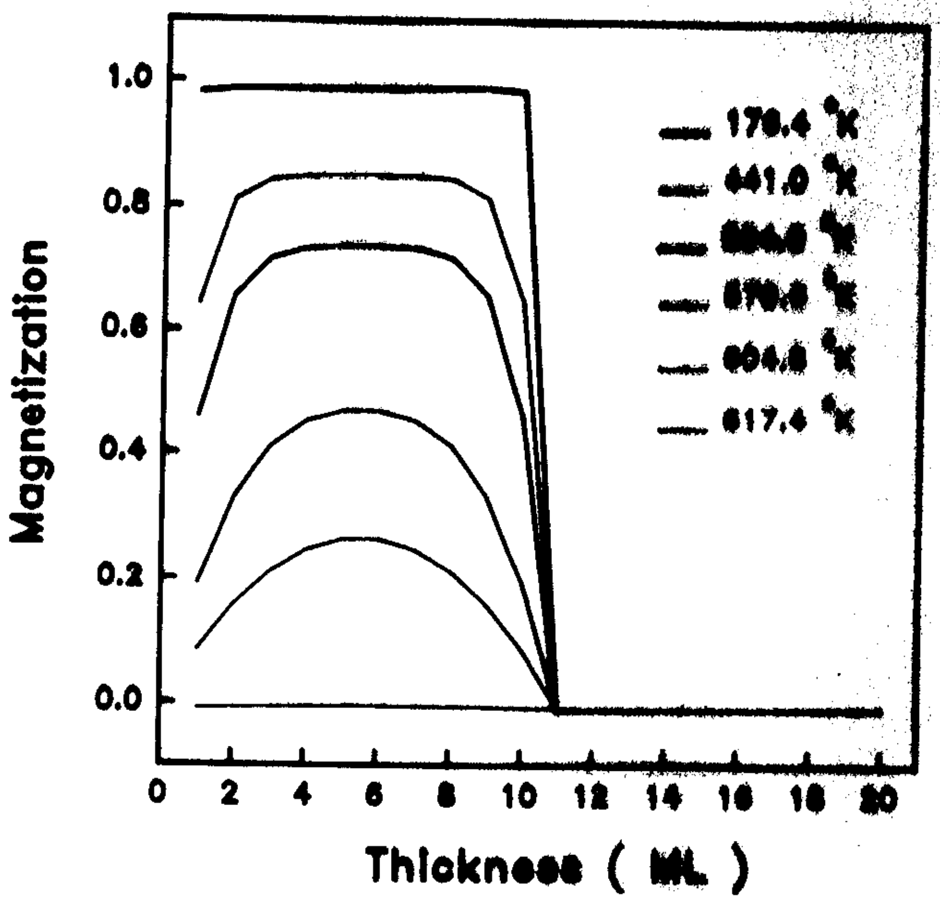

No Intermixing case

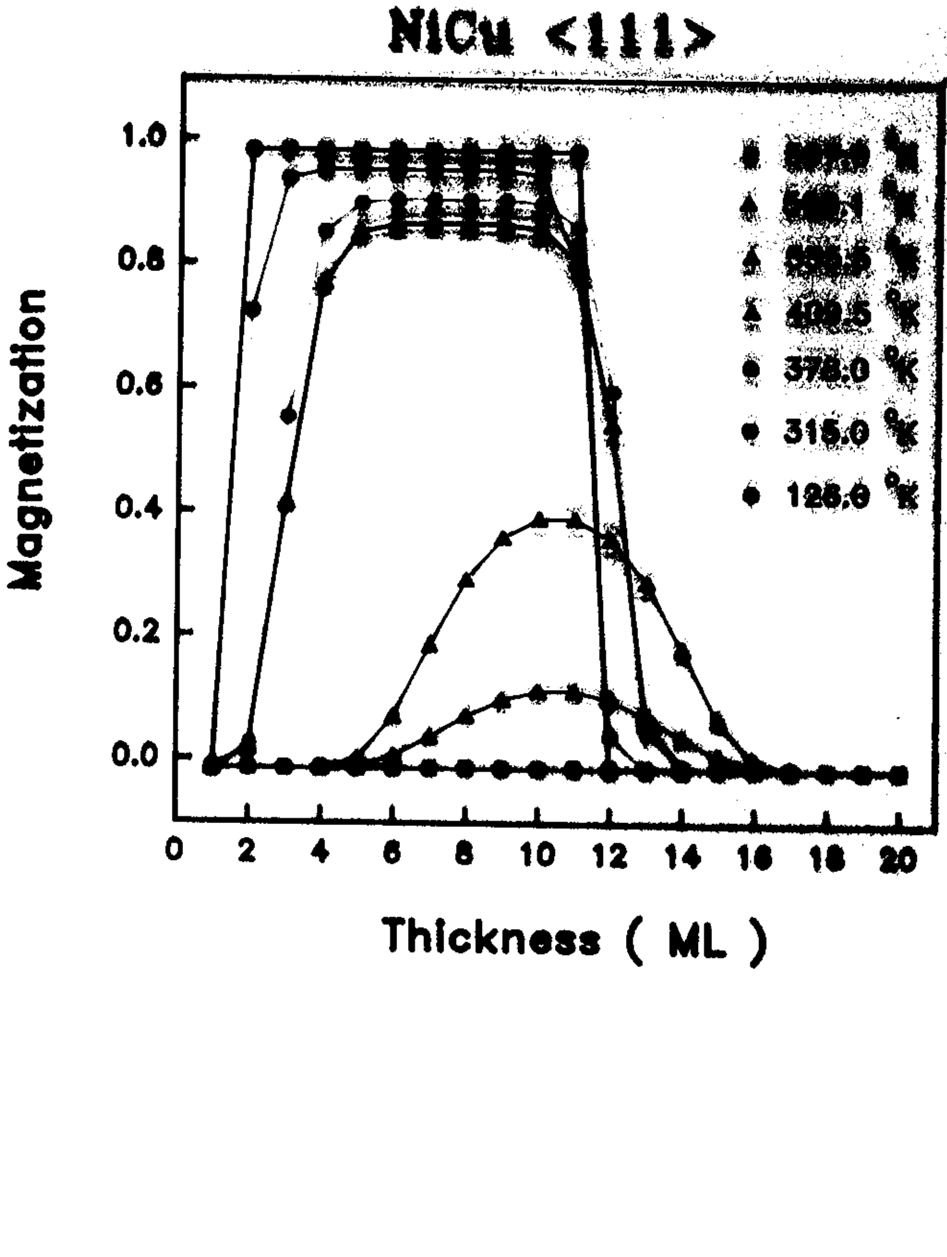
NiCu <111>
Magnetization
1.0
0.8
0.6
0.4
0.2
0.0
0
2
4
6
8
10
12
14
16
18
20
Thickness (ML)
409.5 °K
378.0 °K
315.0 °K
128.0 °K

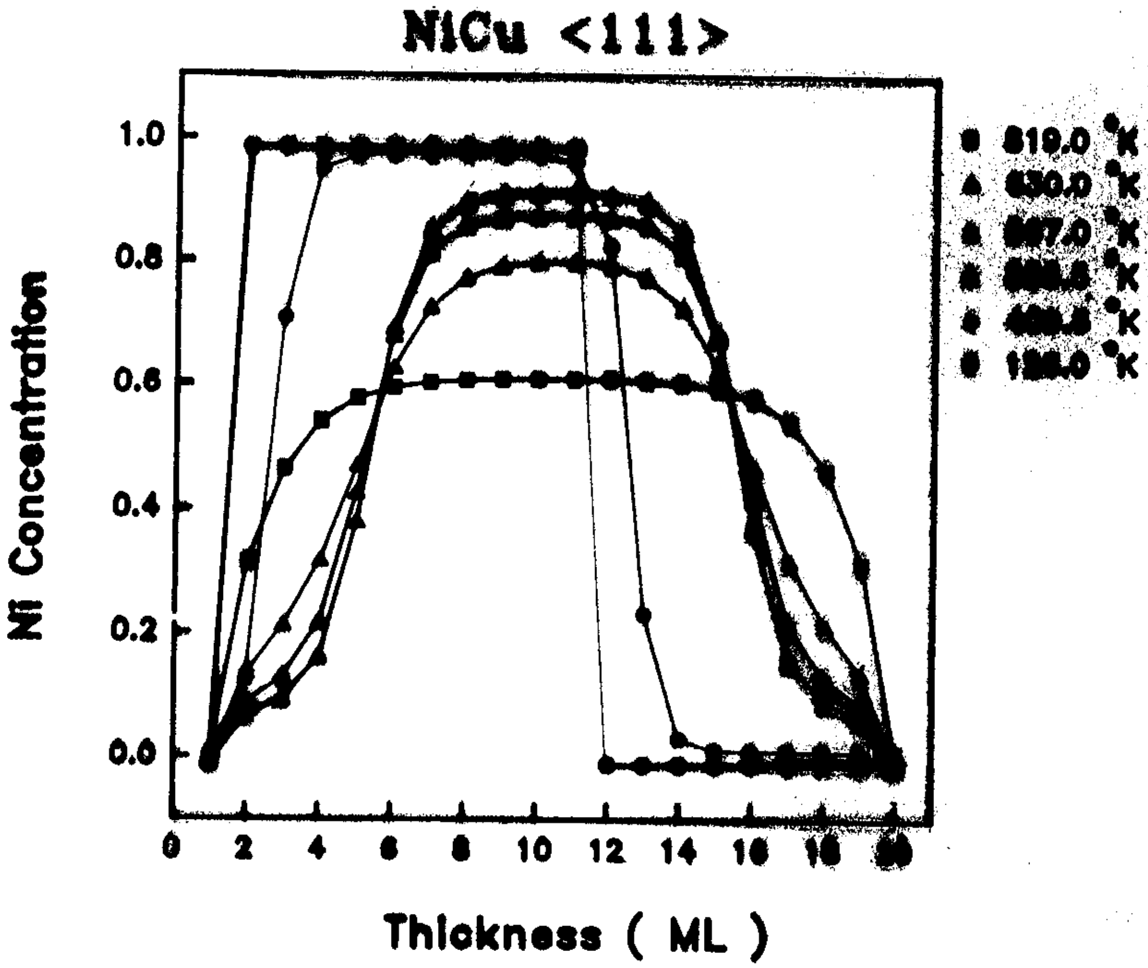

NiCu <111>
Ni Concentration
Thickness (ML)
1.0
0.8
0.6
0.4
0.2
0.0
0
2
4
6
8
10
12
14
16
18
20
819.0 °K
630.0 °K

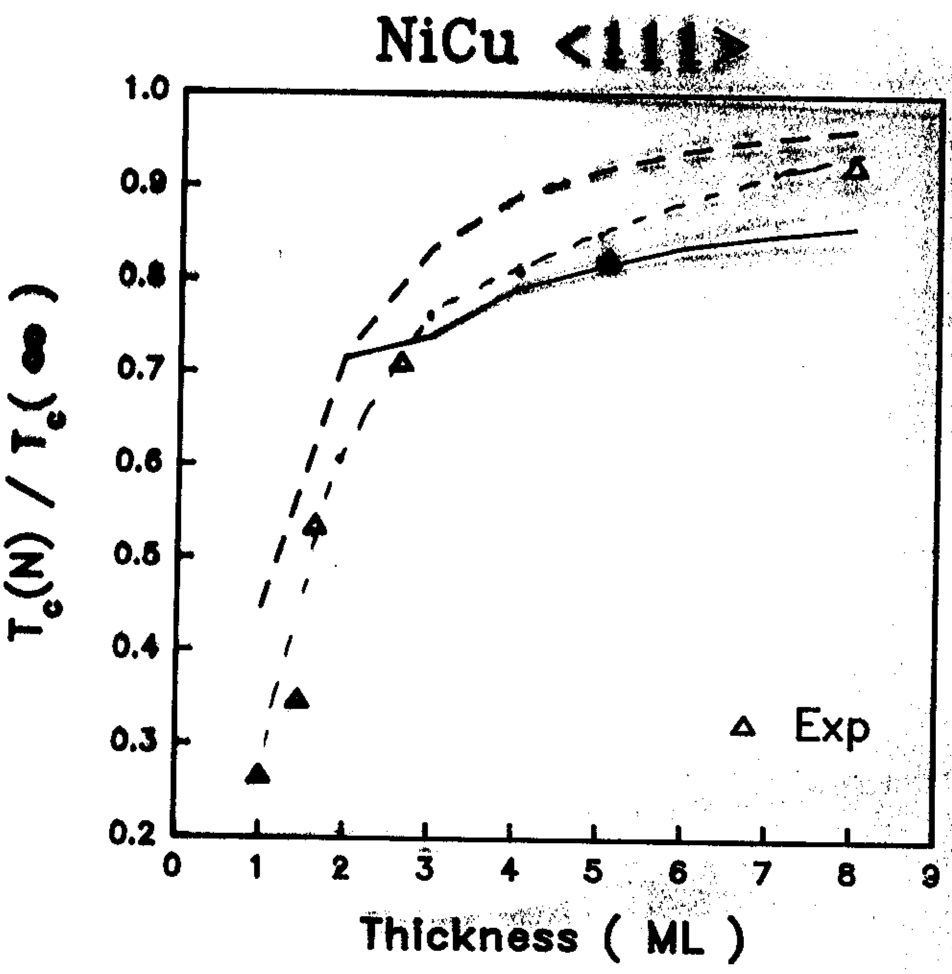

$J_{11} = 0.6\,J$

$J_{12} = 1.38\,J$

$J_{22} = 0.65\,J$